Effect of Lithium ions on structural and magnetic properties of co-precipitated Nickel-Chromium nanoferrite sintered at 1173K for the application of contrast agent in Magnetic Resonance Imaging (MRI)

S. Sukandhiya[1], *B. Uthayakumar[2], R. Roja[3] , S.Periandy[4]

[1,2,3](Research Scholar, Department of Physics, Kanchi Mamunivar center for PG Studies, Puducherry, India.)
[4](Associate Professor, Department of Physics, Kanchi Mamunivar center for PG Studies, Puducherry, India.)
*(Corresponding email id : uthai.kumar@gmail.com)
Corresponding Author: B. Uthayakumar

Abstract: *We are reporting the influence of Lithium ions on the structural and magnetic properties of $Li_xNi_{1-x}Cr_{0.5}Fe_{1.5}O_4$ nanoferrite (x= 0.0, 0.2, 0.4, 0.6 and 0.8) synthesized by Co-Precipitation method with pH as 10. Samples are sintered at 1173K before characterization. The structural properties have been investigated by X-ray Diffraction (XRD) pattern and Fourier Transform Infrared Spectroscopy (FTIR). The morphological observation has been done with Scanning Electron Microscope (SEM) and morphology concurrence with crystallite size obtained from XRD. Elemental compositional stoichiometry has been carried out by Energy Dispersive X-ray Spectroscopy (EDS). The magnetic parameters such as, Saturation magnetization (M_s), Remanence magnetization (M_r), Coercive field (H_c) and Squareness ratio are determined by Vibrational Sample Magnetometer (VSM). XRD pattern revealed the synthesized $Li_xNi_{1-x}Fe_{1.5}Cr_{0.5}O_4$ nanoferrites have the spinel structure with superstructure peaks, at higher concentration of Lithium. Average crystallite size lies between 44nm and 55nm. Saturation Magnetization M_s increases with the increase in Lithium content and for 'x' is 0.6 it is maximum (43.23 emu/gm). Coercivity decreases with the increase in Li^+ ion content and minimum 166.6 Oe for 0.6 concentration. Magnetic Anisotropy constant values decreases with the increase in Lithium content except for 0.2 concentration. Samples with low Li^+ ion concentration have disordered spinel structure of Fd3m space group, which exhibit higher magnetic anisotropy constant. This type of composition releases large amount of heat in the alternating magnetic field and it could be a best candidate for Magnetic Fluid Hyperthermia. When Lithium is low, the intensity of the XRD peaks are more due to higher crystalline nature of the samples. More crystallinity enhances the magnetic anisotropy constant. Higher concentration of Lithium leads to a ordered spinel structure with space group $P4_132$.*

Keywords *- $Li_xNi_{1-x}Cr_{0.5}Fe_{1.5}O_4$, Co-Precipitation method, XRD, SEM, EDAX, FTIR, VSM, Disordered Spinel, Ordered Spinel*

I. Introduction

Today water pollution and air pollution are two of the causes for cancer among people all over the world. The challenge is to diagnose and treat the cancer cells. Emerging novel Nanoferrites solve this problem and it is used in Magnetic fluid hyperthermia for magnetic resonance imaging system and targeted drug delivery system, this induced research community to tailor a best novel nano magnetic material. Magnetic nano spinel ferrite has the potential to produce heat under an alternating magnetic field[1-3]. During magnetization reversal, energy loss occurs. This phenomenon paved the way for promising application of magnetic nano particle in biomedicine, known as Magnetic Fluid Hyperthermia (MFH). MFH plays a vital role in thermal ablation therapy for cancer, since cancerous cells are more sensitive to heat than healthy ones [4,5]. MFH offers a better selectivity as heat is locally generated in the tissue where the magnetic nano particles accumulate. In principle MFH could be conjugated with Magnetic Resonance Imaging (MRI) providing the opportunity to build up a theranostic nano regime to diagnose, treat and monitor the cancer evolution during the therapies [6-7]. Biocompatibility of Magnetite (Fe_3O_4) and Maghemite (γ-Fe_2O_3) attracted this material in nano form for the biomedical applications. Particles with reduced size can be expected to better; it avoids the immunitary system and has a longer circulation time in blood vessels, thus increasing the probability to target the tumor tissue. Nanoparticles are more stable against aggregation, avoiding precipitation and consequently the risk of blood vessel occlusion. A strategy to achieve constant hyperthermic efficiency, a novel combination of nano ferrite with increased magnetic anisotropy is required. Spinel ferrites have the general formula AB_2O_4, where A is a

divalent metal ion (e.g. Co, Mn, Ni and Zn) and B is frequently iron substituted, sometimes with other trivalent metal ions (e.g. Cr, Al, Li and rare earths). The physical and chemical properties of these compounds depend on the distribution of cations between A-sites (tetrahedral) and B-sites (octahedral). To tailor a nano magnetic material with the desired structural and magnetic properties, a fruitful synthesis method, chemical composition, particle size or dopant should be chosen and this can also fine-tuned by changing the nature and amount of substituting element [8].

I.Chicinas et al synthesized Nano crystalline Nickel ferrite by reactive milling method from metal oxides and reported the influence of milling time and impact of annealing. A very disordered Ni-Fe with many defects were obtained by milling, annealing enhances spinel ferrite formation and removes the internal stresses, which results in reduced structural defects [9]. Ramankutty et al synthesized spinel Nickel ferrite, Cobalt ferrite and Copper ferrite nano structures by Co-Precipitation method. They studied the catalytic active behavior and claimed Cobalt nano ferrites is the most active catalyst at lower activation temperature, Copper ferrites is the most active one at higher activation temperature and Nickel is having least activation temperature [10]. S.T.Assar et al studied temperature dependency of the magnetic permeability of and Direct Current conductivity in Li^+ Cobalt-Nickel ferrite and they synthesized it by citrate precursor method. They concluded Li ions enhance electrical and magnetic property of Co-Ni ferrites, when it is at lower concentration [11]. However no information in the literature regarding Lithium doped Ni-Cr nano ferrite. Present research work is to investigate the influence of non-magnetic Lithium on structural and magnetic properties of Nickel-Chromium nano ferrites for better performance in MHF.

II. Materials and Methods

2.1 Material for synthesis

Precursors used in the synthesis process were $LiCl$, $NiCl_2$, $CrCl_3.6H_2O$, $FeCl_3.6H_2O$ and $NaOH$. Analytical grade of these precursors were purchased from SIGMA ALDRICH, Germany with 98% of purity and used in the synthesis without further purification.

2.2 Synthesis Methodology

The physio-chemical properties of nanoparticles are greatly influenced by particle size, crystalline nature, morphology, purity and chemical composition. Using chemical methods, like sol-gel, hydrothermal, co-precipitation and colloid emulsion technique have been conformed to efficiently control the morphology and chemical composition of prepared nano powder. Among these reports of these wet chemical techniques sol-gel, hydro thermal and colloid emulsions are time consuming and involve highly unstable alkoxides and difficult to maintain reaction conditions. From the literature, one of the most flourishing techniques for synthesizing ultrafine nanoparticles with narrow particle size distribution is Co-Precipitation method[9]. These advantages motivated authors to synthesize $Li_xNi_{1-x}Cr_{0.5}Fe_{1.5}O_4$ (x = 0, 0.2, 0.4, 0.6, 0.8) nano ferrites by co-precipitation method. 2M of $FeCl_3.6H_2O$ and 1M of Metal chlorides are made in aqueous solution and they are mixed in stochiometric ratio. Mixture of Aqueous solution is stirred rigorously at 338K for 30 minutes, meanwhile NaOH is added to the brain solution by drop by drop using a burette till solution reaches pH value 10. The required composition of nano ferrites are formed from conversion of metal salt into hydroxide and then transformed into ferrites. The precipitates obtained were thoroughly washed more than three times with double distilled water and acetone. The final product were dried and sintered at 1173 K for the formation of spinel nanoferrite.

III. Result and Discussion

3.1 X - Ray Diffraction analysis

Phase purity, Crystallinity and structural parameters of $Li_xNi_{1-x}Cr_{0.5}Fe_{1.5}O_4$ (x = 0, 0.2, 0.4, 0.8) nanoferrites sintered at 1173K were studied by X-ray diffraction (XRD) patterns. Instrument used to record the XRD pattern is PANalytical-X'Pert PRO powder diffractometer with $CuK\alpha$ radiation (λ=1.544 Å). Fig.1 shows the X-Ray diffraction pattern of the Lithium doped Nickel-Chromium nanoferrite. Peaks in XRD pattern have been indexed as (111), (210), (220), (310), (311), (222), (321), (400), (330), (422), (511), (440), and (620). Comparison of d_{hkl} values as obtained from the X-Ray diffraction data for Li-Cr ferrite JCPDS file No.38-0259 and for Ni ferrite 10-0325 values. All the indexed peaks correspond to characteristic planes. Vertically labeled Peaks (111), (220), (311), (222), (400), (422), (511), (440) and (620) represents the formation of disordered spinel structure of space group Fd3m, with Fe^{3+} at tetrahedral (8a) Wyckoff's positions, and a 1:3 mixture of Li^+ and Fe^{3+} ions at octahedral (16d) positions. Horizontally indexed peaks (210), (310), (321), (330) which reveals the ordered spinel structure of space group $P4_332$ or its enantiomorph $P4_132$ with Fe^{3+} in tetrahedral (8c) and octahedral (12d) sites whereas Li^+ ions occupy the (4b) octahedral positions [10,11]. For 0, 0.2, 0.6 concentration of Lithium shows single phase disordered cubic spinel structure without any secondary phase formation. (111) peak disappeared for the concentration x = 0.6 and 0.8 indicate the composition transforming to ordered spinel. When concentration of Li^+ is highest at 0.8 it result in ordering the spinel crystal structure

and formation is supported with the super structure peaks (210), (310), (321), (330) which reveal, the samples at this concentration having the ordered cubic structure due to the influence of Li^+ ions. Very negligible shifting in the peak position is observed, since Ni^{2+} ion with ionic radius (0.69Å) is replaced with Li^+ ion with ionic radius (0.74 Å). Increase in Lithium content results in the decrease in crystallinity of samples.

Average crystallite is estimated from X-ray reflections indexed (111), (220), (311), (222), (400), (422), (511), (440) and (620), using Scherer's equation [12]. $D = 0.9 \lambda / \beta \cos \theta$ where D is the average crystallite size, β is the full width half maxima, λ is the X-Ray wavelength and θ is the Bragg's angle. Lattice strain of $Li_xNi_{1-x}Cr_{0.5}Fe_{1.5}O_4$ were determined using the Williamson-Hall formula[13, 14]. $\varepsilon = \beta / \tan \theta$ Where ε is the lattice strain of the structure. Lattice constant has been calculated from equation [15] $a = d (h^2 + k^2 + l^2)^{1/2}$ Where 'a' is lattice constant, d be the inter planar distance, hkl is miller indices. X-ray Density can be calculated by [16] $\rho_x = ZM/Na^3$ where Z, M, N and a are the number of molecules per unit cell (here it is 8), Molecular weight of the sample, Avagadro's Number and lattice constant respectively. Dislocation density has been found by using the relation [17]. $\delta = 15 \varepsilon / a D$ Where δ be the dislocation density, all the structural parameters are calculated by the above formulae and tabulated in the Table 1.

From Table 1(a) average crystallite size 'D' estimated for $Li_xNi_{1-x}Cr_{0.5}Fe_{1.5}O_4$ nanoferrites for different 'x' values lie in between 44 nm and 55 nm. Variation in the crystallite size is generally due to the influence of dopant occupancy in the lattice and agglomeration. In the present study average crystallite size varies nonlinearly, this due to migration of Fe^{3+} (0.67Å) ion to tetrahedral site this is possible in nano regime[18]. For concentration x = 0.6 crystallite size is maximum with value of 54.60 nm. This property arise due to more strained and dislocated sub-lattice created by agglomerated magnetic nanoparticles. Lattice constant 'a' of all the samples under investigation have been calculated using the Bragg's equation. Lattice constant value for the Lithium doped Ni-Cr nanoferrite lies in between 8.4400 Å and 8.4800 Å . Higher ionic radius ion Li^+ substitution in place of lower ionic radius Ni^{2+} ion expands the lattice, it results in the increased lattice constant for 0.2, 0.4, 0.6 concentration and obeys Vegard's law. And 0.6 and 0.8 concentration of $Li_xNi_{1-x}Cr_{0.5}Fe_{1.5}O_4$ nano ferrites lattice constant varies non linearly and these compositions violates of Vegard's law which may be due to the deviation of complete normal spinel or complete inverse spinel structure to partially inverted structure. At 0.6 concentration of Li^+, lattice constant decreased, with more strain in the lattice, due to vacancy of oxygen atoms. Molecular weight of the $Li_xNi_{1-x}Cr_{0.5}Fe_{1.5}O_4$ composition decreases with replacement of lower atomic mass (6.938 gm) Li^+ by higher atomic mass (58.69 gm) Ni^{2+} in the composition and this matches with the X-Ray density values calculated from XRD profile. Dislocation density value decreases for x ≥ 0.6 decreases this is due to ordering nature of Li^+ dopant.

3.2 Scanning Electron Microscope (SEM) and Energy Dispersive Spectroscopic (EDS) analysis

SEM micrographs for the synthesized $Li_xNi_{1-x}Cr_{0.5}Fe_{1.5}O_4$ nanoferrites sintered at 1173 K have been captured with the help of VEGA 3 TESCAN for all concentration of the samples. Fig.2 shows morphology of $Li_xNi_{1-x}Cr_{0.5}Fe_{1.5}O_4$ nano ferrite samples for the increase in concentration of Lithium (x = 0, 0.2, 0.4, 0.6, 0.8). The micrographs show the agglomerated grainy structure with clusters of fine particle clinging together. The morphology of surface is almost uniform and regular having cubical to nearly spherical shaped particles for all the concentration except x = 0.8, Replacement of Nickel by Lithium manipulated the morphology. Agglomeration is more for x = 0.6 and this phenomenon is well in agreement with the crystallite size obtained from X-Ray diffraction pattern. At x = 0.2 morphology shows fine particle nature. The surface of the ferrite samples has a number of fine pores or voids that are attributed to the large amount of Oxygen and chlorine gas liberated during the sintering process. Presence of oxygen vacancies results in contraction of Lattice even higher ionic radius dopant is added to the sample. The agglomerated clusters of particles indicate the presence of water molecule between the particles. x = 0.8 concentration only have most agglomerated type of morphology this due to ordering of spinel structure due to the presence of Lithium in higher concentration [19].

EDS spectrum for the $Li_xNi_{1-x}Cr_{0.5}Fe_{1.5}O_4$ (x = 0, 0.2, 0.4, 0.6, 0.8) nanoferrites are recorded with BRUKER EDS and illustrated in fig.3. The result shows that Iron is the major constituent in the composition and Chromium is the next major constituent to the iron in the sample. The peak values remain constant with a very small variation due to it stochiometry for all the concentration. The values of Nickel vary with the increase in Lithium concentration. Peak for Lithium is not obtained because Silicon detector used in Energy Dispersive X-Ray spectroscope for the present study is not having sensing nature to detect the energy emitted by very small lithium ion, which is having K shell for transition for auger electron.

3.3. Fourier Transform Infrared Spectroscopy (FTIR) Analysis

FTIR spectra of $Li_xNi_{1-x}Cr_{0.5}Fe_{1.5}O_4$ nanoferrites at various concentration of 'x' are recorded with SHIMADZU FTIR Spectrometer and illustrated in Fig 4. Peak values of FTIR spectra for all samples tabulated in Table 2. Two intense absorption bonds within the range of 600-400 cm^{-1} are observed, which are correspond to tetrahedral (A) group and octahedral (B) group[20, 21]. From the Table 2 Intrinsic stretching vibration

frequency of metal-oxygen at tetrahedral site observed in a range 620 cm^{-1} to 570 cm^{-1} and its value shifting with the increase in concentration of Li$^+$ in the samples. Metal-oxygen stretching vibration at octahedral site is revealed by peaks obtained in between 444 cm^{-1} and 410 cm^{-1}. This is due to the ordering phenomena in spinel structure by the dopant and it matches with the result obtained from XRD. Band lies in between 495 cm^{-1} and 483 cm^{-1} assigned to metal ion-oxygen complexes in the octahedral sites [22-26]. Shift in the band position is due to the variation in the cation-Oxygen bond length of the octahedral and tetrahedral sites of the spinel structure. Displacement of Ni^{2+} ions by larger Li$^+$ in octahedral sites in Lithium doped Nickel-Chromium ferrite results in a slight increase in metal oxygen bond length and consequently decrease the wave number of octahedral and tetrahedral sites by increasing substitution content [27, 28]. Intensity of octahedral and tetrahedral bonds increases for x ≤ 0.4 and with the addition of Li$^+$ content again intensity decreases for 0.6 and 0.8 concentration of dopant values. It is well known that the intensity ratio is function of change of dipole moment with the internuclear distance. This value represents the contribution of ionic bond Fe-O in the lattice. So the observed increase and decrease in the absorption band intensity with increase in Lithium content, is due to perturbation occurring in Fe-O bonds. The electronic distribution of Fe-O bonds greatly affected by the dopant Li$^+$ which is having comparatively bigger radius and low atomic weight [29].

3.4 Vibrational Sample Magnetometer (VSM) analysis

Magnetization as a function of the applied magnetic field (hysteresis loops) for Li$_x$Ni$_{1-x}$Cr$_{0.5}$Fe$_{1.5}$O$_4$ nanoferrites (x = 0, 0.2, 0.4, 0.6, 0.8) recorded with LAKESHORE Vibrational sample magnetometer at 300 K and applied field of 20 KOe are shown in Fig.5. Magnetic parameters saturation magnetization (M$_s$), Remanence Magnetization (M$_r$), Coercivity (H$_c$), Squareness ratio and Magnetic anisotropy constant (K) are obtained from Hysteresis loop and tabulated in Table 3. The value of anisotropy constant was calculated from Stoner-Wohlfarth relation as follows [30] H$_c$ = K/M$_s$ Where H$_c$ is the coercivity , M$_s$ saturation magnetization and K is magnetic anisotropy constant. Generally magnetic properties in the prepared sample arise from coupling between spin and orbital angular momentum (L-S coupling) and electron spin (S-S coupling) [31]. In the case of spinel nano magnetic ferrite material magnetic parameters are influenced by cation distribution, collinearity and non-collinearity (canting) of spins on their surface, Crystallite size and dopant.

In present study all the concentration of Li$^+$, the hysteresis loops show similar behaviour where the magnetization first increases abruptly with increase in the field up to 1000 Oe and then increase slowly and saturate nearly 2500 Oe of the applied magnetic field. Saturation magnetization value increases with the increase in crystallite size and decreases with decrease in the crystallite size. This phenomenon is in agreement with the previous works. Coercivity increases at the 0.2 concentration of Li$^+$, for all other concentrations Coercivity value decreases with the increase in Lithium value. But Remanence value increase with increase in Li$^+$ ion. This is due to more number of incorporation of non-magnetic Lithium ion on the sublattices . All the sample shows super-paramagnetic behaviour. The appearance of super-paramagnetism indicates that the magneto crystalline anisotropy, which is important to hold magnetic ions in certain direction, has been overcome by thermal energy [32]. The magnetic anisotropy constant is maximum for the concentration 0.2 and in this crystallinity is more with no superstructure peaks are obtained. From these results magneto crystalline anisotropy is more for high crystallinity sample. And high crystallinity is possible in disordered spinel structure. Ordered spinel structure have low value of magnetic anisotropy constant. Thus VSM result matches with XRD and FTIR findings.

IV.   Conclusion

Li$_x$Ni$_{1-x}$Cr$_{0.5}$Fe$_{1.5}$O$_4$ (x = 0, 0.2, 0.4, 0.6, 0.8) nanoferrites with novel composition were successfully synthesized by easy and simple co-precipitation method with average crystallite size between 44nm and 55 nm. All physical properties are studied for samples sintered at 1173K. Addition of Li$^+$ ion influenced the structural properties such as average crystallite size, lattice constant, lattice strain, dislocation density and X-Ray density of the synthesized samples. Superstructure reflection peaks from XRD analysis suggest that nano crystal lattice transform disordered to ordered spinel structure in the higher concentration of the dopant. SEM shows morphology manipulated by Li$^+$ ion in the sample. From VSM analysis and Low concentration of Li$^+$ induced magnetic ordering and crystal disordering. At higher concentration Lithium induced most ordered spinel structure and disordered magnetic structure which is found from the magnetic anisotropy constant value. Important finding in this work is 0.2 concentration of Lithium in Ni-Cr has its maximum magnetic anisotropy constant value, which will release more thermal energy in alternating magnetic field, and should be act as best candidate for magnetic fluid hyperthermia and in targeted drug delivery system.

References

[1] G. Dixit, J.P.Singh, R.C.Srivastava, H.M. Agrawal, Magnetic resonance study of Ce and Gd doped $NiFe_2O_4$ nanoparticles, *J. Magn. Mater. 324* (2012) 479-483.

[2] M.A.Iqbal, M. Islam, M.N. Ashiq, I.Ali, A. Iftikhar, H.M. Khan, Effect of Gd-substitiution on physical and magnetic properties of $Li_{1.2}Mg_{0.4}Gd_xFe_{(2-x)}O_4$ ferrites, *J.Alloy compd. 579* (2013) 181-186.

[3] P. Samoila, T.Slatineanu, P. Postolache, A.R.Iordan, M.N. Palamaru, The effect of chelating/combustion agent on catalytic activity and magnetic properties of Dy doped Ni-Zn ferrite, *Mater.Chem. Phy. 136* (2012) 241-246.

[4] A.I. Borhan, P. Samoila, V.Hulea, A.R. Iordan, M.N. Palamaru, Effect of Al^{3+} substituted zinc ferrite on photocatalytic degradation of Orange I azo dye, *J. Photochem. Photobiol. A: Chem, 279* (2014) 17-23.

[5] I. Sharifi, H. Shokrollahi, S.Amiri, Ferrite-based magnetic nanofluids used in hyperthermia applications, *J.Magn. Magn. Mater. 324* (2012) 903-915.

[6] T.N.Brusentsova, V.D. Kuznetsov, Synthesis and investigation of magnetic properties of substituted ferrite nanoparticles of spinel system $Mn_{1-x}Zn_x[Fe_{2-y}L_y]O_4$, *J.Magn. Magn. Mater. 311* (2007) 22-25.

[7] P. Mathur, A.Thakur, M. Singh, Impact processing and polarization on dielectric behavior of $Ni_xMn_{0.4-x}Zn_{0.6}Fe_2O_4$ spinel ferrites, *Int. J. Mod. Phys. B 23(11)* (2009) 2523-2533.

[8] A. Thakur, P. Mathur, M. Singh, Controlling the properties of Mn-Zn ferrites at high frequency by substituting In^{3+} and Al^{3+} ions, *Indian J. Pure Appl. Phys. 46* (2008) 47-53.

[9] T.F.Marinca, I.Chicinas, O.Isnard, V.Pop, F.Popa. Synthesis, structural and magnetic characterization of nano crystalline Nickel ferrite obtained by reactive milling. *J.Alloys and Compounds, 509* (2011) 7931-7936.

[10] C.G. amankutty, S.Sugunan, *J. App. Catal.A: Gen 218*, 39 (2001)

[11] S.R.Dhage, Y.Khollam, S.B.Deshpande, V.Ravi, Co-precipitation technique for the preparation of nanocrystalline ferroelectric $SrBi_2Ta_2O_9$, *Mater.Res.Bull.38* (2003) 1601-1605.

[12] A.Tomas, P.Laruelle. J.L Dormann, M.Nogues, *Acta Crystallogra. C39* (1983) 1615-1617.

[13] E.Wolska, P.Piszora, J.Darul, W.Nowicki, *Mater.Sci.Forum 378-381* (2001) 551-556.

[14] S.Rahman, K.Nadeem, M.Anis-ur-Rehman, M.Mumtaz, S.Naeem, I.Letofsky-Papst, *Ceramic International 39* (2013) 5235-5239.

[15] G.K.Williamson, W.H.Hall , *Acta Metall. 1* (1953) 22.

[16] W.Chen , W.W.Wu, S.Q.Liu, J.W.Xu, D.S.Liu, X.H.Wu, Y.Zhou, J.Wu, *Mater.Sci.Semicond.Process.39* (2015) 544.

[17] P.B.Belavi, G.N.Chavan, L.R.Naik, R.Somashekar, R.K.Kotnala, *Materials Chemistry and Physics 132* (2012) 138-144

[18] R.C.Kumbale, P.A Sheikh, S.S.Kamble and Y.D.Kolekar, " Co-Zn and Mn-Zn Ferrite Nanoparticles prepared by Coprecipitation", *Journal of Magnetism and Magnetic Materials, 288*, 2005, pp. 470-477.

[19] S.Prabahar, and M.Dhanam, CdS thin films from two different chemical baths-structural and optical analysis, *J.Cryst.Growth, 285*, No.1-2, 41 (2005).

[20] N.Ponpandian and A.Narayanasamy, *Journal of applied Physics 92* (2000) 2770-2778.

[21] C.Julien, M.Massot, *Mater. Sci. Eng. B 100* (2003) 69.

[22] J.C.Bernier, P.Poix, A.Michael, *Bull.Soc.Chim. Fr.138* (1963) 1661.

[23] Y.P.Fu, Y.D.Yao, C.S.Hsu, *Journal of Alloys and Compounds 421* (2006) 136.

[24] A.M.Shaikh, S.A.Jadhav, S.C Watawe, B.K, Chougule, *Journal of Material letters 44* (2000) 192.

[25] A.Pradeep, G.Chandrasekaran, *Journal of Material Letters 60* (2006) 371-374.

[26] P.Priyadarhini, A.Pradeep, P.S.Rao, G.Chandrasekaran, *Materials Chemistry and Physics 116* (2009) 207.

[27] A.G.Boshale, B.K.Chougule, *Material Chemistry and Physics 97* (2006) 273.

[28] J.Smit and H.P.J ijn, *Ferrite,* 1959.

[29] S.E.Shirsath, B.G.Toksha, R.H.Kadam, S.M.Patange, D.R.Mane, G.S, Jangam, A.Ghasemi, *J.Phys.Chem.Solids 71* (2010) 1669.

[30] N.Singh, A.Agrawal, S.Sanghi, P. Singh, *Physica B 406* (2011) 687.

[31] M.A.Gabbal, Y.M.A. Angari, *Mater.Chem.Phys.118* (2009) 153.

[32] A.Verma, T.C.Goel, R.G.Mendiratta, P.Kishan, *Journal of Magn. Magn. Mat. 208*,(2000) 13-19.

[33] C.Liu, B.Zou, Adam J.Rondinone, and Z.J.Zhang, *Jorunal of American Chemical Society 122* (2000) 6263-6267.

TABLE 1: Structural parameters of $Li_xNi_{1-x}Cr_{0.5}Fe_{1.5}O_4$ for various concentrations sintered at 1173K

Li content 'x'	Composition	Crystallite Size D (nm)	Lattice Constant a (Å)	Molecular Weight g/mole	X-ray density g/cm^3	Lattice strain 10^{-3}	Dislocation Density 10^{15}
0.0	$Ni_{1.0}Cr_{0.5}Fe_{1.5}O_4$	44.70	8.4407	232.405	5.1340	2.48	1.68
0.2	$Li_{0.2}Ni_{0.8}Cr_{0.5}Fe_{1.5}O_4$	50.56	8.4729	222.055	4.8497	2.31	0.87
0.4	$Li_{0.4}Ni_{0.6}Cr_{0.5}Fe_{1.5}O_4$	49.70	8.4866	211.7042	4.6013	3.59	4.32
0.6	$Li_{0.6}Ni_{0.4}Cr_{0.5}Fe_{1.5}O_4$	54.60	8.4453	201.354	4.4408	1.85	0.62
0.8	$Li_{0.8}Ni_{0.2}Cr_{0.5}Fe_{1.5}O_4$	44.20	8.4880	191.003	4.1493	2.37	1.11

TABLE 2: Vibrational frequency of tetrahedral and octahedral sites

Li content 'x'	Composition	$\nu_{1\ tetra}$ cm^{-1}	$\nu'_{1\ tetra}$ cm^{-1}	$\nu_{2\ octa}$ cm^{-1}	$\nu'_{2\ octa}$ cm^{-1}
0.0	$Ni_{1.0}Cr_{0.5}Fe_{1.5}O_4$	614.01	495.76	443.25	-
0.2	$Li_{0.2}Ni_{0.8}Cr_{0.5}Fe_{1.5}O_4$	618.13	496.81	441.32	-
0.4	$Li_{0.4}Ni_{0.6}Cr_{0.5}Fe_{1.5}O_4$	613.98	-	443.46	-
0.6	$Li_{0.6}Ni_{0.4}Cr_{0.5}Fe_{1.5}O_4$	609.51	-	-	416.37
0.8	$Li_{0.8}Ni_{0.2}Cr_{0.5}Fe_{1.5}O_4$	571.38	483.09	-	409.24

TABLE 3: Magnetic parameters of $Li_xNi_{1-x}Cr_{0.5}Fe_{1.5}O_4$ for various concentrations sintered at 1173K

Li content 'x'	Composition	M_s (emu/g)	M_r (emu/g)	H_c (Oe)	M_r/M_s	K (erg/cm^3)
0.0	$Ni_{1.0}Cr_{0.5}Fe_{1.5}O_4$	29.21	13.21	316.5	0.4522	9244.965
0.2	$Li_{0.2}Ni_{0.8}Cr_{0.5}Fe_{1.5}O_4$	30.76	19.98	322.1	0.6495	9907.28
0.4	$Li_{0.4}Ni_{0.6}Cr_{0.5}Fe_{1.5}O_4$	43.15	25.96	188.8	0.6015	8147.22
0.6	$Li_{0.6}Ni_{0.4}Cr_{0.5}Fe_{1.5}O_4$	43.23	28.59	166.6	0.6613	7201.08
0.8	$Li_{0.8}Ni_{0.2}Cr_{0.5}Fe_{1.5}O_4$	16.57	08.90	211.0	0.5368	3497.36

M_s - Saturation magnetization; M_r - Remanent Magnetization; H_c – Coercivity; K - Magneto Crystalline Anisotropy;
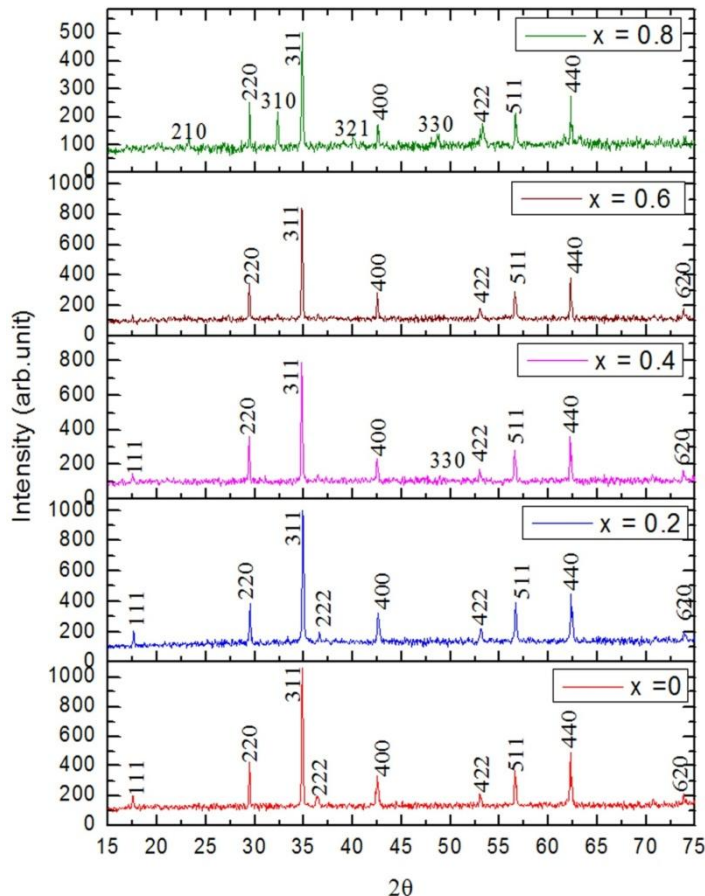
Figure 1: X-Ray Diffraction pattern of Li Doped Ni-Cr nano ferrite samples
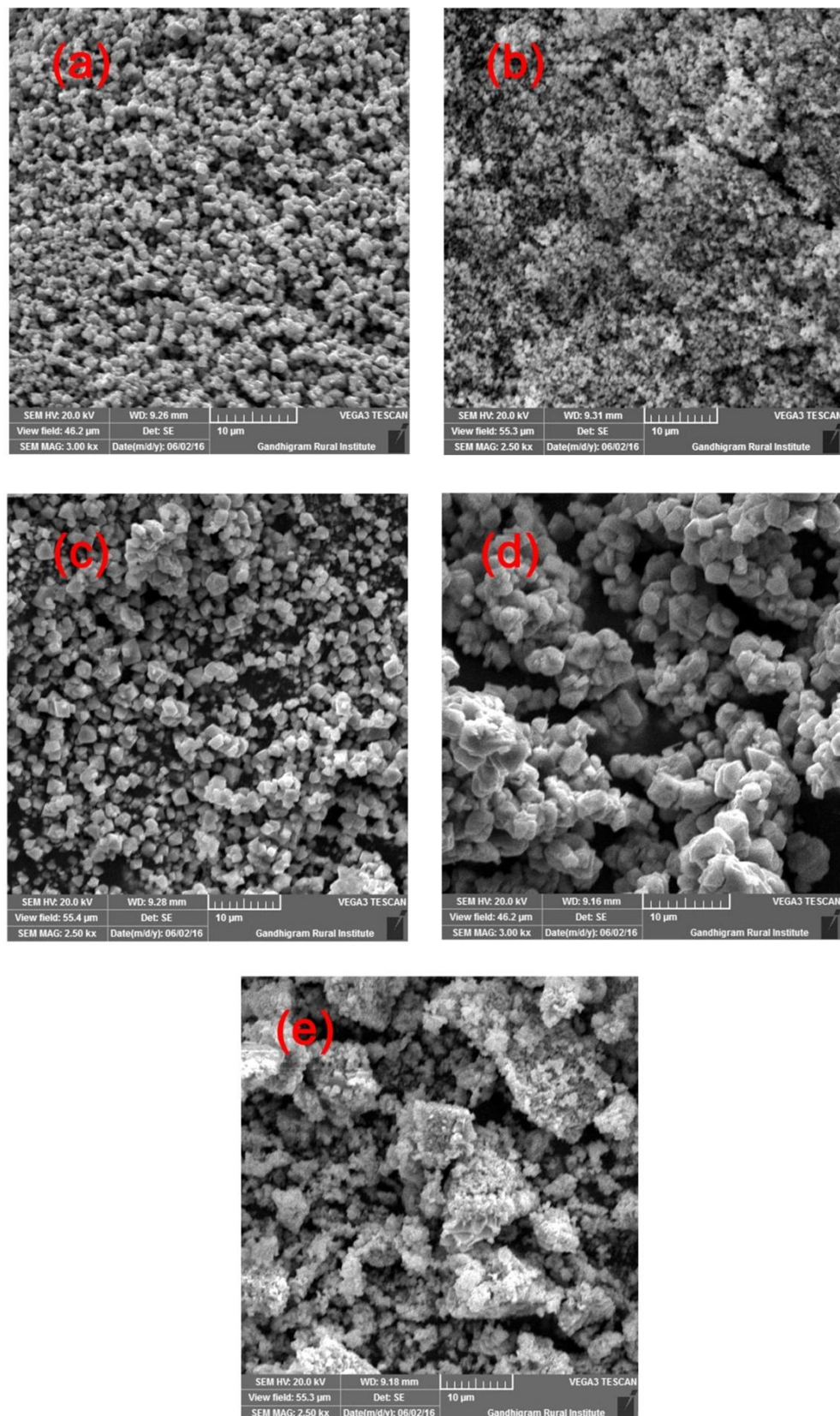
Figure 2. SEM micrograph of $Li_xNi_{1-x}Cr_{0.5}Fe_{1.5}O_4$ (x= 0(a), 0.2(b), 0.4(c), 0.6(d), 0.8(e)) nanoferrite sintered at 1173K
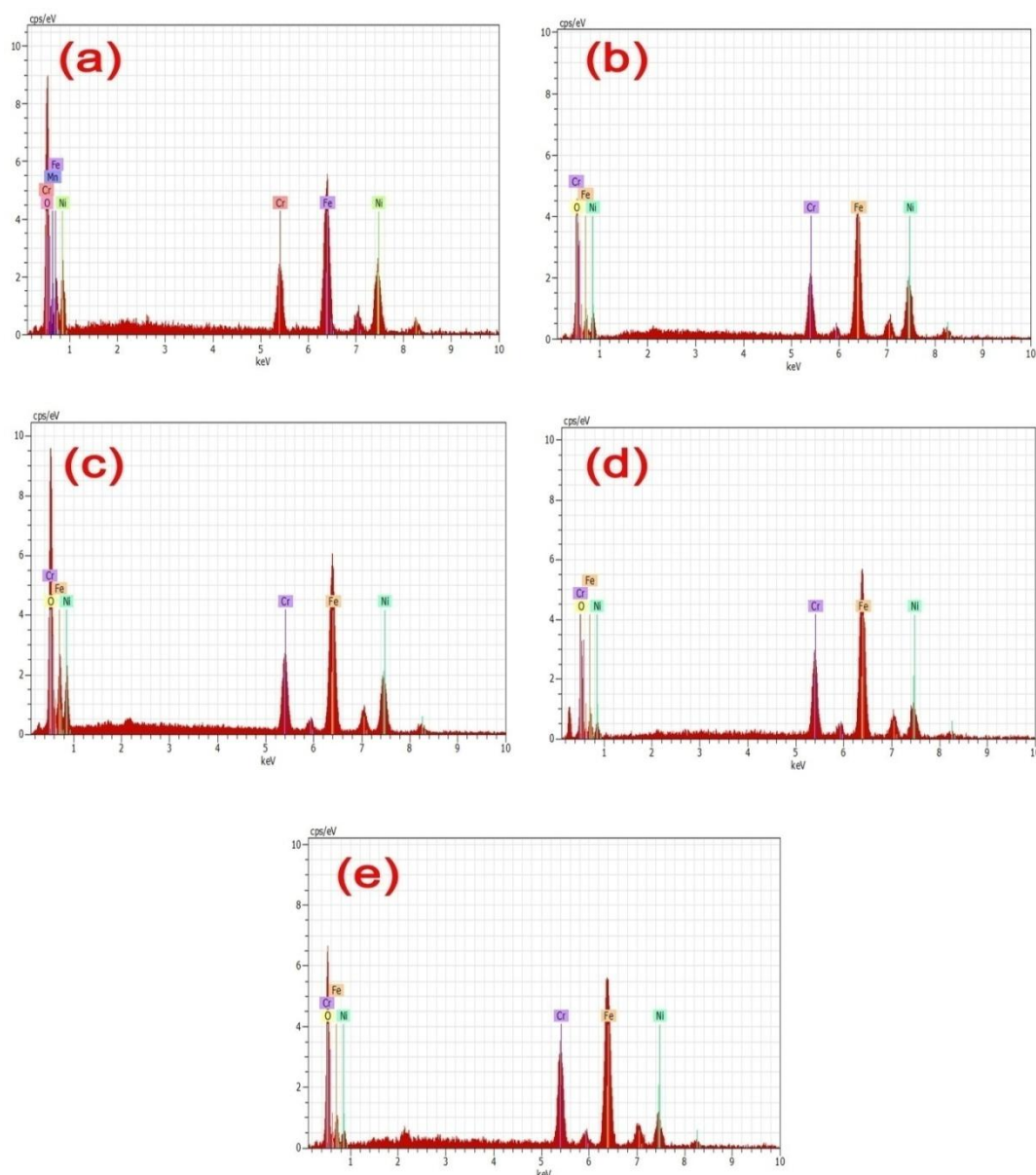
Figure 3. EDS of $Li_xNi_{1-x}Cr_{0.5}Fe_{1.5}O_4$ (x= 0(a),0.2(b), 0.4(c), 0.6(d), 0.8(e)) nanoferrite sintered at 1173K
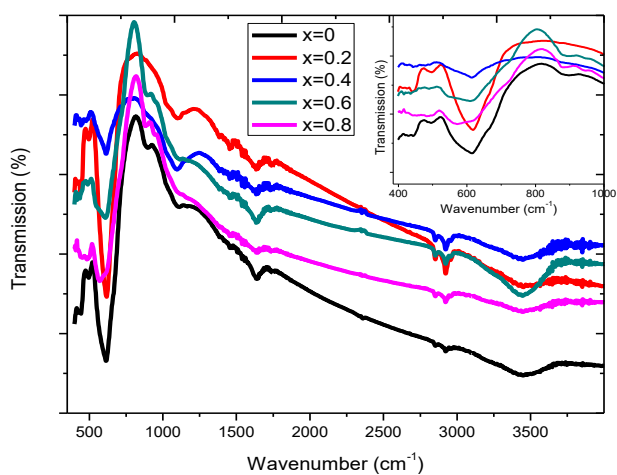
Figure 4. FTIR spectra of $Li_xNi_{1-x}Cr_{0.5}Fe_{1.5}O_4$ (x= 0,0.2, 0.4, 0.6, 0.8) nanoferrite sintered at 1173K
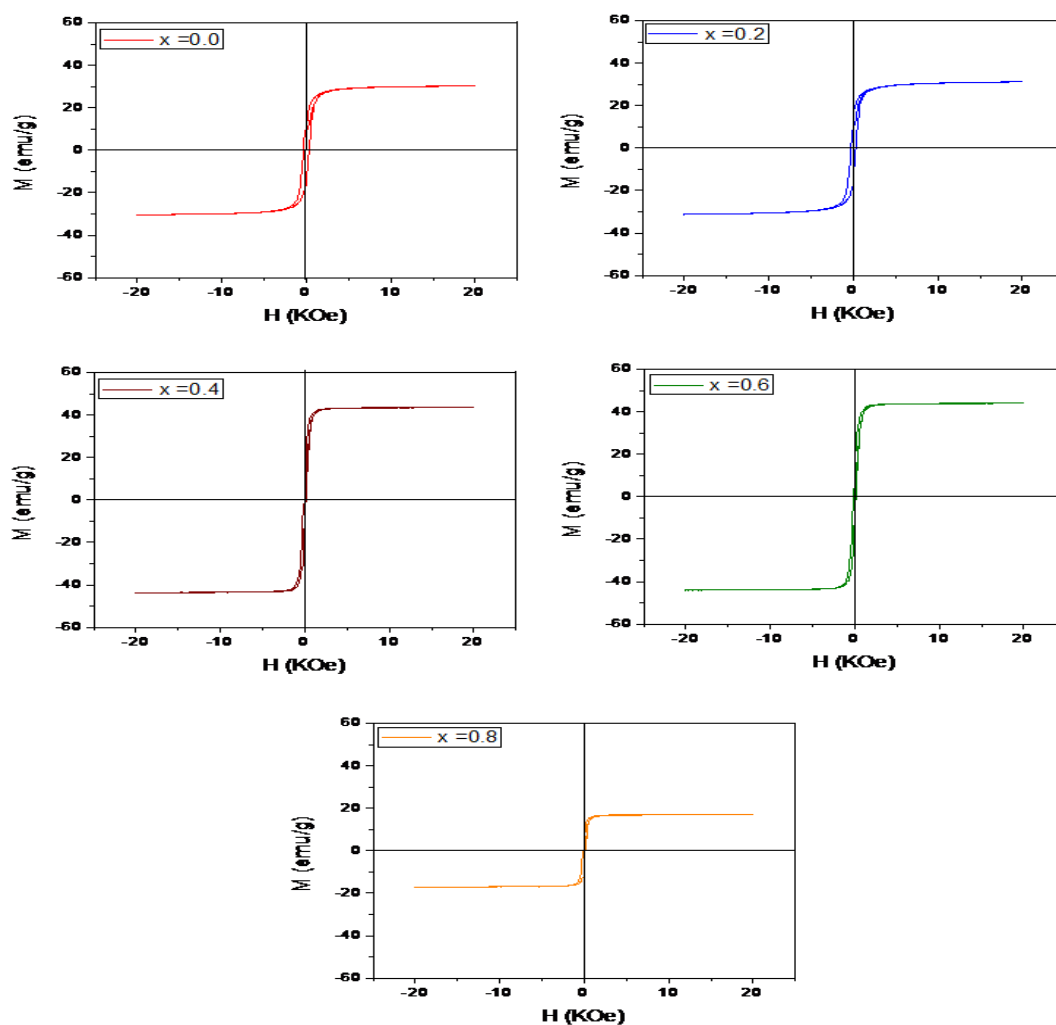
Figure 5. Magnetic hysteresis curves of $Li_xNi_{1-x}Cr_{0.5}Fe_{1.5}O_4$ (x= 0,0.2, 0.4, 0.6, 0.8) sintered at 1173K

S. Sukandhiya. "Effect of Lithium ions on structural and magnetic properties of co-Precipitated Nickel-Chromium nanoferrite sintered at 1173K for the application of contrast agent in Magnetic Resonance Imaging (MRI)." IOSR Journal of Applied Physics (IOSR-JAP), vol. 9, no. 5, 2017, pp. 52–60.